Geographical and temporal trends in southern African clear-sky, solar ultraviolet-B flux: 1979 to 2001

Charles F. Musil[a*], Greg E. Bodeker[b,c], Malcolm W.J. Scourfield[c] and Leslie W. Powrie[a]

Geographical and temporal trends in clear-sky, biologically active ultraviolet-B (UV-B, 280–315 nm) radiation were modelled from 23-yr satellite ozone records across latitudes 22°S to 35°S and longitudes 16°E to 34°E in southern Africa. Modelled values were calibrated against broadband and spectral instrument-based measurements and mapped at 2.6-km^2 resolution in accordance with the internationally accepted UV-index scale. Statistically significant latitudinal, longitudinal and intra-annual UV-index gradients were evident, the latitudinal gradients especially displaying large seasonal anomalies ranging from a 4.5% increase in UV-index per degree reduction in latitude during winter to a 0.5% increase in summer. Inter-annual UV-index gradients seemingly corresponded with the 11-yr cycle of extraterrestrial solar activity in which peak UV-indices (up to 13% deviation from 23-yr averages) appeared associated with years of least solar activity, though there were exceptions. These UV-index peaks were most prominent between midwinter and early spring in July, August and September. They also displayed geographical anomalies, the largest deviations in UV-indices mostly apparent at high latitudes and low longitudes. Inter-annual UV-index gradients mostly exceed UV-index increases induced by anthropogenic emissions of ozone-depleting trace gases over the 23-yr assessment period. The latter increases, though relatively modest (up to 9% between 1979 and 2001), have caused substantial geographical alteration in the distribution of indices across South Africa, with midday clear-sky UV-indices of magnitude 13 and greater corresponding to 72% of the country's interior in December 2001 compared with only 2% under comparable levels of solar activity in December 1979. Such geographical shifts are expected to intensify with continuing ozone depletion, especially at the next solar cycle minimum anticipated in 2007/08.

Introduction

The decline in stratospheric ozone at both high and mid-latitudes in the northern and southern hemispheres due to anthropogenic emissions of ozone-depleting trace gases[1] has raised concerns about the detrimental effects that increased amounts of biologically active ultraviolet-B (UV-B: 280–315 nm) radiation reaching the Earth's surface may have on human health and other biological systems.[2] Such increases in ambient sunlight have recently been reported at various sites across the world,[3,5] but it is unclear how these will be distributed globally in the future.[6]

In southern Africa, definitive measurements of solar ultravio-let-B irradiance at ground level are presently restricted to broadband and spectral instrumentation operated by the School of Pure and Applied Physics at the University of Natal in Durban, and a Solar Light UV-B Biometer network maintained by the South African Weather Service, which also manages a Global Atmospheric Watch Station at Cape Point linked to a baseline surface radiation network station at De Aar. However, many of the instrument-based measurements of solar UV-B irradiance from these locations are of insufficient uniformity and/or extent for a combined analysis of long-term geographical and temporal trends across southern Africa. Indeed, given the high spatial and temporal variability of surface UV radiation, and the difficulty of maintaining calibration within networks of instruments, it seems unlikely that satisfactory long-term UV trends can be derived from ground-based monitoring stations alone. In contrast, satellite-based observations of the atmosphere provide adequate spatial coverage, as well as nearly continuous long-term monitoring, but the derivation of surface UV-irradiance by such means is indirect, since satellite instruments detect radiation reflected only by the atmosphere and Earth's surface.

Radiative transfer models that integrate transmission, reflection and atmospheric absorption present a viable alternative to ground- and satellite-based UV-irradiance measurements, and these have been applied extensively to estimate past variability in biologically active UV-B irradiance from satellite ozone records and predict future UV-B irradiance from cyclic signals underlying the variability in the total column ozone.[6] In southern Africa, estimates of past and future variation in erythemal active UV-B irradiance have been confined to the five cities of Cape Town, Port Elizabeth, Bloemfontein, Durban and Johannesburg.[7] Notably lacking are modelled estimates of erythemal UV-B irradiance for the entire southern Africa region, their validation against instrument-based measurements and their expression in a form simply understood by both scientists and the general public. In this regard, the UV-index scale was accepted by the international scientific community at the World Health Organization/World Meteorological Organization (WHO/WMO) meetings held in Les Diablerets during 1995 and 1997 as the fundamental parameter for familiarizing the public with the detrimental effects of UV on human health, particularly in relation to skin damage, sunburn times and proper use of sunscreens. Both the WMO, WHO and United Nations Environment Programme promote harmonized use of the UV-index scale globally. They advise governments to employ this as an educational tool in their health promotion programmes, and encourage dissemination channels such as the media and tourism industry to publish UV-index forecasts and promote sun-warning messages.

In view of the above, and the need to convey guidelines on permissible sun exposure times to the southern African public, we modelled and mapped surface UV-B irradiances across southern Africa consistent with the UV-index scale, calibrated these against instrument-based measurements to provide realistic indices, and analysed geographical and temporal trends over a 23-year assessment period.

Methods

Modelled UV-indices

Daily estimates of clear-sky solar UV-B irradiance at solar noon (midday) covering the period 1 January 1979 to 31 December 2001 were obtained at a resolution of ~2.6 km^2 across latitudes 22°S to 35°S and longitudes 16°15′E to 33°45′E, using a modified computer-based empirical model[8] integrated with Geographic Information Systems (GIS). The modelled UV-B irradiances at

[a]Research and Scientific Services, National Botanical Institute, Private Bag X7, Claremont 7735, South Africa.

[b]National Institute for Water and Atmospheric Research, Lauder, Central Otago, New Zealand.

[c]School of Pure and Applied Physics, University Natal, Durban 4041, South Africa.

*Author for correspondence. E-mail: musil@nbict.nbi.ac.za

1-nm step size in the 280–315 nm UV-B range were weighted by the International Commission for Illumination (CIE) reference erythemal action spectrum,[9] integrated over wavelength, and converted to UV-indices (erythemal-weighted UV-B irradiance in W m^{-2} × 40). Digitized data inputs into the empirical model included geographical coordinates for each 1.6 × 1.6-km grid element, dates, South African Standard Times (SAST) compliant with solar noon, altitude above sea level (median value in each group of 64 × 200 m^2 grids due to the general bias of the median towards the mean in asymmetric records), relative humidity near to midday (long-term average at 14:00 SAST) interpolated from meteorological records, as well as total column ozone concentration in Dobson units (DU). Ozone concentrations, extracted from 1° latitude by 1° 15′ longitude grid data using bilinear (weighted average of four surrounding grid points) interpolation (applying piecewise polynomials), were obtained from the NASA Total Ozone Mapping Spectrometer (TOMS) instrument flown on board the Nimbus 7,[10] Meteor 3,[11] Earth Probe[12] and Adeos[13] satellites, and the Global Ozone Monitoring Experiment (GOME) flown on the ERS-2 satellite.[14] Owing to the different satellite orbits, sampling close to local midday was every 24 h for TOMS and every 72 h for GOME. A rural environment and a ground cover corresponding to green farmland were presumed in all model computations. The paucity of suitable records of cloud abundance and form in the meteorological archives as well as the high spatial heterogeneity and short-term temporal variability in these factors precluded their inclusion in the model. The same rationale applied to atmospheric aerosol concentrations, and a default value representing typical atmospheric aerosol levels in a rural environment (aerosol scattering coefficient ≈ visual range >3.192 km) was applied. The impact of the incompletely accounted for temporal and spatial variations in atmospheric aerosols, as well as relative humidity, on model sensitivity was relatively minor (approximate 1% and 0.2% alterations in erythemal-weighted UV-B irradiance per 10% change in visual range and relative humidity, respectively), and resolved partly by calibrating the modelled UV-irradiances against simultaneous instrument-based measurements over an extended period in an industrialized coastal city under humid conditions.

Instrument-measured UV-indices

Daily UV-irradiance measurements were obtained concurrently with broadband and spectral instrumentation located in an observation tower, which allowed full view of the horizon, situated on top of the School of Pure and Applied Physics building at the University of Natal in Durban (29°58′S; 30°57′E). Measurements taken with the broadband instrument covered a 2617-day period from 1 March 1993 to 30 April 2000. Those taken with the spectral instrument covered a much shorter 1277-day period from 1 November 1996 to 30 April 2000, and assisted in correcting the broadband measurements for ozone dependency, a consequence of slight wavelength mismatches between broadband meter spectral responses and biological action spectra.[15]

The broadband instrument comprised an internally temperature-stabilized pyranometer (YES model UV-B1, Yankee Environmental Systems, Inc., Turners Falls, MA) operated in accordance with the manufacturer's standards,[16] which was checked against an unused reference YES pyranometer at approximately six-month intervals. The instrument's analogue voltage output was interfaced with a data logger, which digitized and averaged readings recorded every 15 s over 5-min intervals. The effective standard time of each averaged analogue voltage reading was assigned at the centre of the 5-min recording

interval. Averaged analogue voltage readings were downloaded daily into a personal computer programmed to compute corresponding solar zenith angles (SZA), convert voltage readings into biologically weighted irradiances, compliant with the CIE reference erythemal action spectrum,[9] and convert these to UV-indices.

The spectral instrument comprised a double monochromator spectroradiometer (Bentham model DM 150, Bentham Instruments Ltd, Reading, Berkshire) interfaced with a personal computer. The instrument's stepper-motor-driven gratings covered the spectral range 290–500 nm with a bandwidth of 1 nm and a scanning duration of 180 s. The light sensor was a fibre-optic cable topped by a Teflon diffuser connected to a temperature-stabilized photomultiplier detector sealed in an insulated container. Instrument calibration was performed monthly. Absolute response was checked against an incandescent lamp (Bentham CL2, Bentham Instruments) mounted inside a baffled cylinder to exclude ambient and reflected lamplight. Wavelength alignment was checked against vapour emission lines from a mercury arc lamp. The spectroradiometer was programmed to commence measurements at dawn and perform scans at intervals of 5-degree SZA throughout the day. Standard times were assigned to the centre effective wavelength of the integrated spectra. Absolute spectral irradiance measurements were biologically weighted with the CIE reference erythemal action spectrum,[9] integrated over the 280–315 nm wavelength range and converted to UV-indices.

Calibration of modelled against measured UV-indices

UV-index measurements (2246 with the YES and 1125 with the Bentham instruments), excluding those ignored (371 YES and 152 Bentham) as a result of instrument performance and calibration checks, taken in close proximity to midday were matched for date, time and SZA with those computed by the empirical model. The criteria applied in this matching process were that the effective standard times and corresponding SZA values assigned to the modelled UV-indices, and those measured with the YES and Bentham instruments deviated by no more than 60 s in duration and 0.25° in SZA. The matched UV-indices (1482 YES and 955 Bentham) were then date coordinated with digitized measurements of daily sunshine duration obtained from a Campbell-Stokes type recorder operated by the South African Weather Service at a proximate (7 km distant) meteorological station at Durban International Airport. Of these, 286 YES and 192 Bentham measured UV-indices corresponded to days with sunshine periods exceeded 90% of total day length (effectively clear-sky conditions).

Data synthesis and statistical analysis

Least-squares regressions of the empirical-modelled UV-indices against the broadband and spectral instrument-measured UV-indices provided mathematical functions for calibration of the modelled UV-indices, that is, their adjustment to conform to the realistic instrument-measured values. A Student's t-test assessed the regression slopes for statistical significance.

Following their adjustment, the modelled UV-indices were mapped, and reduced to a resolution of ~2340 km^2 by averaging these across 0.5° latitude × 0.5° longitude grid elements. This process simplified statistical analyses, yet maintained adequate precision for testing temporal differences in UV-indices along spatial gradients. A generalized linear model analysis of variance (S-Plus 4.5 Professional Release 2, Lucent Technologies) tested the responses of the modelled
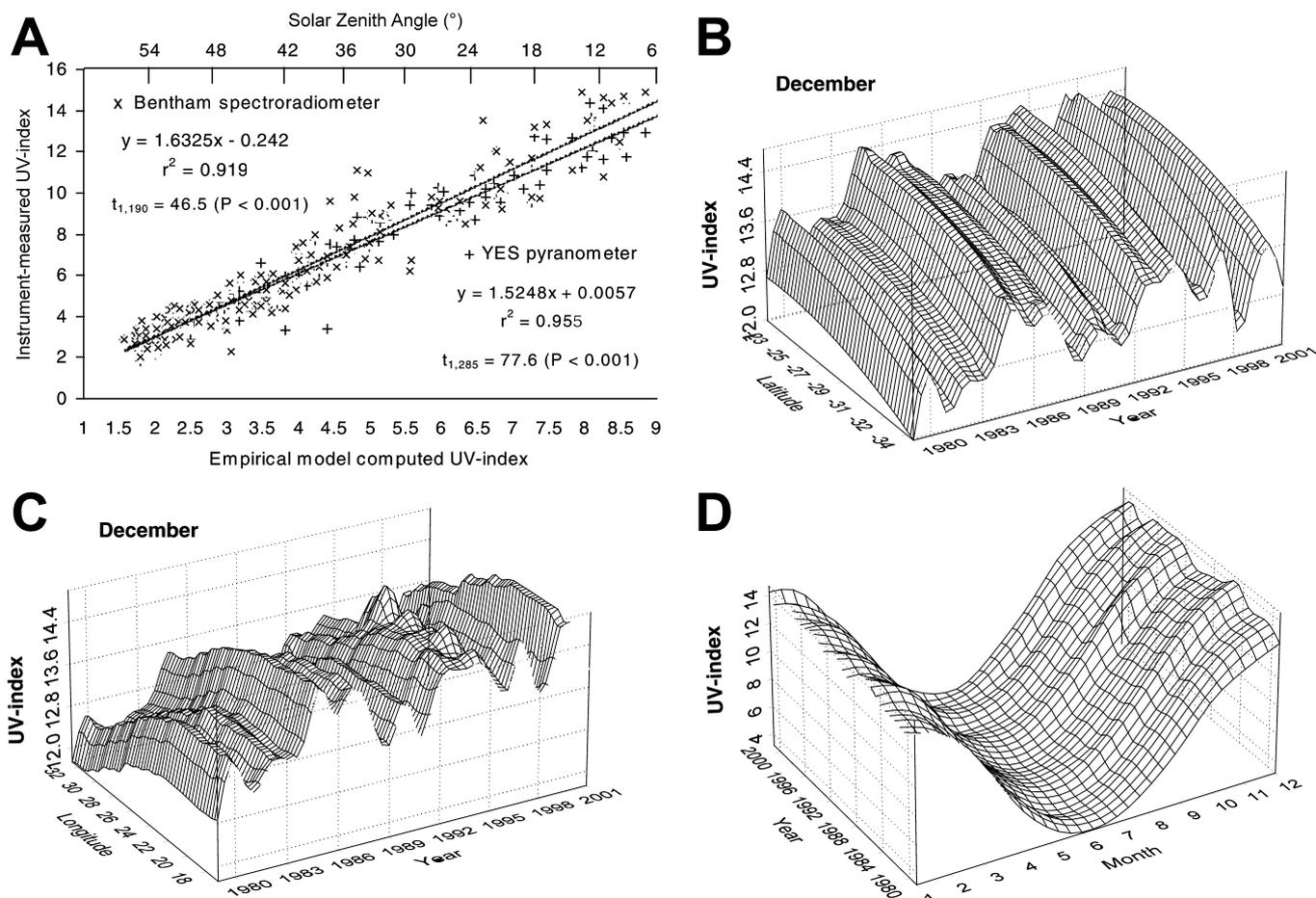
Fig. 1. **A**, Empirically modelled versus broadband and spectral instrument-measured UV-indices at midday under clear skies; **B**, latitudinal; **C**, longitudinal and **D**, monthly fluctuations in these UV-indices over a 23-yr (1979–2001) assessment period.

UV-indices to the fixed effects of year, latitude, longitude and their combinations. Tests were conducted on both the monthly and annually averaged UV-indices. A Duncan's multiple range test[17] separated UV-indices that differed significantly ($P \geq 0.05$) in magnitude inter-annually. These UV-indices were expressed as percentage deviations from the 23-yr average to compensate for natural cyclic oscillations in surface UV-B irradiance. The following formula was applied:

$$\text{UV-index deviation } (\%) = \frac{(\text{Mean 23-yr UV-index } - \text{ UV-index}) \times 100}{\text{Mean 23-yr UV-index}}.$$

The overall increases in monthly and annually averaged UV-indices over the 23-yr assessment period were quantified using least-squares regressions, and these were tested for significance with a classical analysis of variance.

Results and discussion

Numerous studies have confirmed theoretical relationships under cloud-free and low-aerosol sky conditions between ozone reduction and UV-B increases,[18–20] and under known total column ozone modelled UV-B irradiances have also been reported to fall within the experimental errors of both broadband meters[21] and spectroradiometers.[22–24] Our empirical-modelled UV-indices were significantly ($P \leq 0.001$) correlated both over discrete and wide solar zenith angles with the broadband and spectral instrument-measured values but were of consistently smaller magnitude (Fig. 1A). Their adjustment to conform to realistic instrument values was executed by quantify-

ing their relationship with the combined broadband and spectral instrument-measured UV-indices ($y = 1.5693x - 0.0966$; $r^2 = 0.937$; $t_{1,477} = 84.4$, $\approx P \leq 0.001$). Correction of the broadband instrument measurements for ozone dependency reduced error margins by only a small fraction ($2.40 \pm 0.44\%$).[15] It was noteworthy that the adjusted UV-indices compared auspiciously with instrument-measured values reported by independent observers for other locations in southern Africa. For example, our adjusted indices modelled for clear skies at Windhoek (22°34′S; 17°06′E, 1725 m) at midday between December 1999 and January 2000 were in the range 15.5 to 15.9, which were equivalent to indices in the range 15 to 16 measured at this location over the same period.[25]

Analysis of our modelled UV-indices confirmed the existence of significant ($P \leq 0.05$) spatial gradients across southern Africa (Table 1). The main geographical trends were significantly ($P \leq 0.05$) increased indices (Table 1) with decreasing latitude (Fig. 1B), decreasing longitude (Fig. 1C) and increasing altitude above sea level (Fig. 2A). Latitudinal UV-index gradients displayed large seasonal anomalies, ranging from a 4.5% increase in UV-index per degree reduction in latitude during June to a 0.5% increase in December. Longitudinal UV-index gradients were relatively smaller in magnitude and displayed little seasonal variation, ranging from a 0.7% increase in UV-index per degree reduction in longitude during June to an 0.8% increase in December. Vertical UV-index gradients were in the order of a 6.2% increase in UV-index per 1000 m elevation above sea level.

Modelled spatial gradients in surface UV-B irradiance have
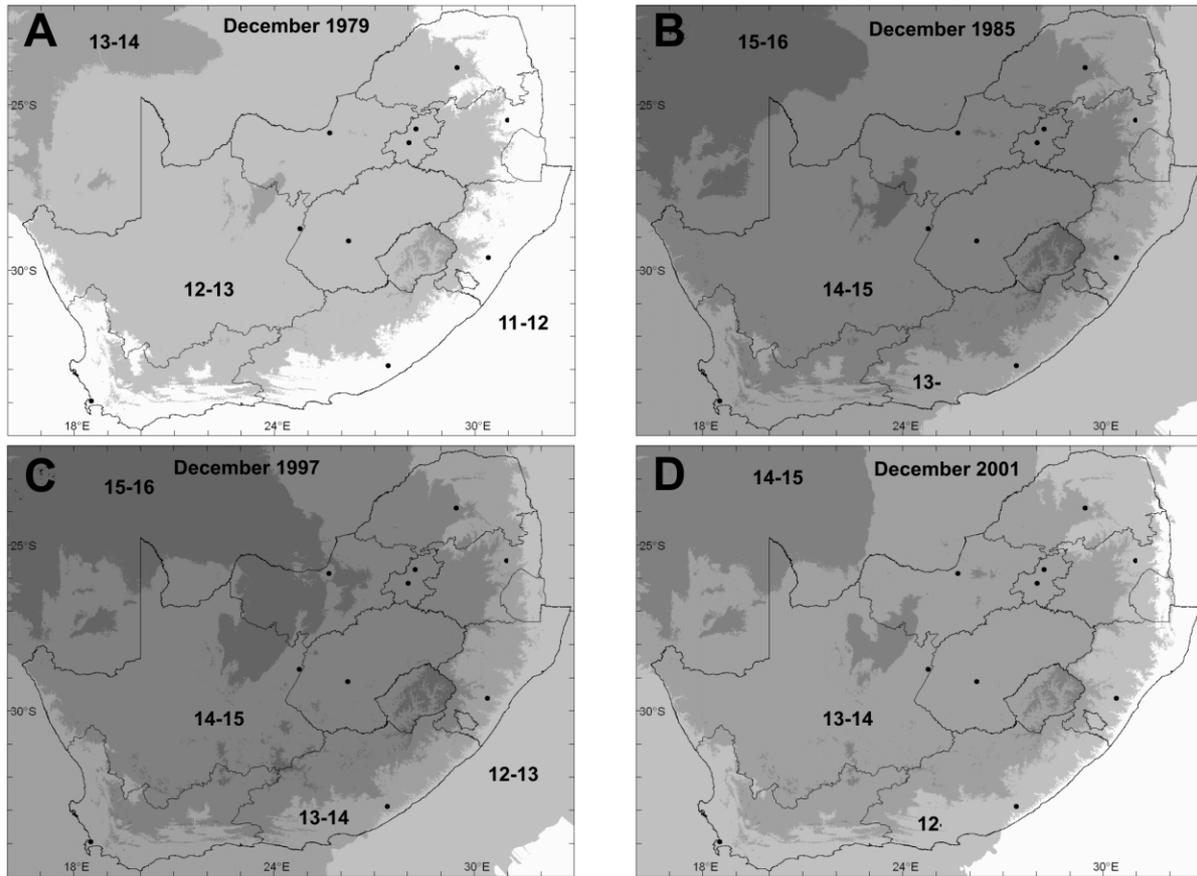
	% of land area within RSA			
UV-index	1979	1985	1997	2001
11–12	26.9			3.9
12–13	71.1	4.0	5.2	23.9
13–14	2.0	23.6	22.4	67.5
14–15		68.9	61.9	4.8
15–16		3.5	10.6	

Fig. 2. Modelled distribution of midday, clear-sky UV-indices across southern Africa during periods of maximum solar cycle activity in (**A**) December 1979 and (**D**) December 2001, and during periods of minimum solar cycle activity in (**B**) December 1985 and (**C**) December 1997.

been corroborated by instrument-based measurements. For example, the Robertson-Berger meter network in the United States has confirmed higher erythemal-damaging UV-B irradiances at lower latitudes,[26–28] and other R-B-type meter measurements in Russia,[29] Switzerland,[30] Malaysia[31] and New Zealand[23] have also substantiated such broad latitudinal differences in erythemal UV-B irradiance. Also, spectral measurements have

shown higher summertime values of UV-A and UV-B radiation in the southern hemisphere, for instance at Lauder (New Zealand) and Melbourne (Australia), than at comparable latitudes in the northern hemisphere, such as at Nuremberg (Germany).[22,24] These disparities between southern and northern hemispheres have been attributed to the yearly cycle of the Sun–Earth distance, lower stratospheric ozone levels in the

Table 1. *F*-ratios ($F_{1,19726}$) from generalized linear model analyses of variance and least-squares regressions of monthly and annually averaged UV-indices over a 23-yr assessment period.

Month	Generalized linear model ANOVA							Least-squares regression
	Year: 1979–2001	Latitude: 22–35°S	Longitude: 16–34°E	Year × Latitude	Year × Longitude	Latitude × Longitude	Year × Latitude × Longitude	
Jan	**3386.0*****	**11899.0*****	**13661.6*****	**14.3*****	**9.7****	**13.3*****	<0.1	**1437.2*****
Feb	**2312.3*****	**58119.2*****	**9569.2*****	**48.9*****	**21.3*****	**32.2*****	<0.1	**503.6*****
Mar	**4.2***	**178515.7*****	**11169.8*****	**33.4*****	3.2	**104.8*****	<0.1	0.4
Apr	**18.4*****	**238383.6*****	**7381.5*****	**25.9*****	2.0	**159.5*****	<0.1	1.3
May	**17.5*****	**316858.9*****	**5616.9*****	**16.2*****	0.8	**221.9*****	<0.1	0.9
Jun	**1478.0*****	**618878.6*****	**7403.0*****	**96.9*****	0.1	**385.7*****	<0.1	**43.2*****
Jul	**2601.7*****	**371482.7*****	**4601.6*****	**79.4*****	0.6	**209.4*****	<0.1	**129.6*****
Aug	**4508.2*****	**216319.7*****	**5311.4*****	**62.6*****	**4.0***	**150.0*****	<0.1	**368.2*****
Sep	**5802.3*****	**162109.0*****	**12206.4*****	**18.8*****	**19.9*****	**165.8*****	<0.1	**589.4*****
Oct	**2887.8*****	**50457.1*****	**12876.6*****	< 0.1	< 0.1	**65.3*****	<0.1	**685.5*****
Nov	**2375.5*****	**19674.8*****	**21149.8*****	1.11	3.2	**30.8*****	<0.1	**773.7*****
Dec	**2885.0*****	**3901.7*****	**14152.7*****	0.3	0.6	**7.5****	<0.1	**1474.4*****
Annual	**4801.6*****	**213690.0*****	**23941.6*****	**20.1*****	1.9	**170.4*****	<0.1	**353.1*****

Significant effects at * $P \le 0.05$, ** $P \le 0.01$ and *** $P \le 0.001$ are presented in bold type.

Table 2. Annually averaged extraterrestrial solar flux, and monthly and annually averaged UV-index deviations from 23-year averages.

Year	Solar flux at 2000 MHz	UV–index deviation (%)												
		Jan	Feb	Mar	Apr	May	Jun	Jul	Aug	Sep	Oct	Nov	Dec	Annual
1979	191.6	−0.5f	0.5j	−0.7efg	−5.2b	−8.4b	−6.2a	−4.9bc	−7.2ab	−7.3ab	−4.1d	−8.4a	−7.8a	−5.0a
1980	198.4	−7.0a	−6.3a	−1.4de	0.7de	2.7ghi	2.2ef	3.1ghi	2.3f	0.5f	1.1i	2.1j	−0.1h	−0.0e
1981	202.6	−0.7f	−2.1de	−1.9cd	0.0de	−0.8de	−1.3cd	−10.1a	−8.7a	−6.6b	−6.1c	−4.8b	−5.8b	−4.1b
1982	174.8	−3.2cd	−2.7c	−5.8a	−5.4b	−7.7b	−7.2a	−4.0bcd	−1.1d	−1.9d	0.1gh	−2.4d	−2.6e	−3.7bc
1983	119.9	−3.9b	−2.4cd	0.0fgh	1.2de	0.5efg	−3.4bc	−4.6bcd	−6.5b	−4.0c	−4.4d	−1.8e	−2.5e	−2.6cd
1984	100.9	−0.6f	−1.4fg	0.6hi	−3.2c	−1.7cde	−1.9cd	−2.2de	−4.1c	−1.8d	−3.1e	1.6ij	0.2h	−1.5e
1985	74.8	0.9h	**4.8m**	3.8k	3.4fg	**4.6ij**	**4.6fgh**	**4.5hi**	**7.7h**	**4.5hi**	**6.4m**	**5.5m**	**6.2o**	**4.7l**
1986	73.9	**4.9n**	2.4k	**5.5l**	**4.4fgh**	**5.6jk**	**4.2fgh**	**4.8i**	−3.7c	−1.1de	0.0gh	2.0j	0.9gi	2.5jk
1987	85.3	2.4k	3.3l	1.9j	−0.2d	0.6efg	−1.4cd	−0.7ef	−0.5de	−0.3ef	0.3h	1.0h	4.5m	0.9ij
1988	141.1	−0.1g	−1.0gh	4.2k	2.9fg	0.2def	−2.6cd	−3.0cde	−1.6d	−3.7c	−1.3f	−2.2de	−1.9f	−0.9ef
1989	213.4	−3.3c	−0.5hi	−0.9def	−5.8b	−2.0cd	−6.6a	−9.5a	−8.7a	−8.5a	−7.7b	−3.0c	−3.6d	−5.0a
1990	189.8	−2.9d	−3.6b	−2.8c	0.4de	1.8fgh	3.6fg	**5.4i**	**5.5g**	**7.1j**	3.3jk	0.5g	1.1i	1.6fghi
1991	208.0	3.2m	2.2k	−2.0cd	3.3fg	3.7hij	0.1de	−3.7cd	−6.7b	−4.2c	−9.5a	−4.7b	−4.5c	−1.9d
1992	150.1	−1.9e	−1.7ef	−1.6de	3.4fg	**7.5k**	**6.4h**	**4.1hi**	**8.4hi**	**7.4j**	**8.0n**	3.5l	2.3j	**3.8k**
1993	109.6	1.7j	−1.5fg	1.8j	**5.1h**	**4.7ij**	−1.0cd	3.2ghi	1.8f	2.9g	**4.9l**	2.6k	3.3k	2.5jk
1994	85.6	2.6kl	1.0j	0.2gh	1.8ef	–	**4.9fgh**	0.4f	2.1f	−2.2d	−2.3e	1.4hi	–	1.0fgh
1995	77.2	–	–	–	–	–	–	1.9fgh	1.0ef	3.6gh	−0.7fg	0.1g	3.7l	1.6k
1996	72.0	1.3i	2.5k	1.0hij	0.4de	−3.6c	−1.0cd	−6.4b	−2.2cd	1.0f	1.2i	−0.9f	−0.6	−0.6fgh
1997	80.9	1.8j	1.0j	1.4ij	**5.6h**	3.6hij	**5.7gh**	**12.9k**	**10.0ij**	**4.6hi**	3.7k	**5.5m**	**6.3o**	**5.2l**
1998	118.1	**6.0o**	**4.6m**	**5.3l**	**4.0gh**	**4.2hij**	2.9fg	0.8fg	−6.0b	−4.4c	−2.6e	−2.1de	−3.8d	0.8ghi
1999	152.9	−1.7e	−3.9b	−4.4b	−5.5b	−6.7b	3.3fg	**8.8j**	**11.7j**	**6.0i**	2.9j	0.4g	0.3h	0.9fgh
2000	178.8	−1.8e	−0.1i	−4.7b	−11.5a	−11.0a	−5.5ab	2.1fgh	1.8f	**5.3i**	3.4jk	2.7k	**5.0n**	−1.2ef
2001		2.9l	**5.1m**	0.5hi	0.4de	2.2fgh	−0.0de	−3.0cde	**4.6g**	3.1g	**6.2m**	1.5hi	−0.7g	1.9kj
1979–2001		**4.3**	3.5	0.1	0.4	0.44	**4.2**	**6.9**	**9.0**	**7.9**	**5.7**	**4.0**	**4.8**	**4.3**

Values within each column followed by the same letter are not significantly different from each other at $P \leq 0.05$, with those exceeding 4% presented in bold type.

southern hemisphere, and higher tropospheric pollutants (ozone and aerosols) in Germany. As regards vertical UV-index gradients, measurements at remote locations in Chile have confirmed increases in biologically effective UV-B irradiance of 4–10% per 1000 m elevation above sea level, which is in agreement with model calculations for unpolluted air. However, other locations display much larger vertical UV-B irradiance gradients, for example, up to 40% increase in UV-B per 1000 m elevation above sea level near Santiago, Chile,[32] and between 9 and 23% in the Swiss Alps,[33] these presumably being due to more tropospheric ozone and atmospheric aerosols at lower elevations at these locations.

Analyses also revealed significant ($P \leq 0.05$) temporal gradients. Intra-annual UV-index gradients (up to 300% UV-index increase) between winter and summer (Fig. 1D) exceeded by several orders of magnitude inter-annual gradients (Table 2). The latter seemingly corresponded with the 11-yr cycle of extraterrestrial solar activity in which peak UV-indices (largest deviations from 23-yr averages) were mostly associated with periods of least solar activity, for instance years 1985 and 1997, though there were exceptions, such as years 1990 and 1999 (Table 2). These UV-index peaks were most prominent between mid-winter and early spring in July, August and September and also displayed significant ($P \leq 0.05$) geographical anomalies (temporal versus spatial interactions), though not in all months of the year (Table 1). These anomalies were reflected in inconsistent geographical patterns of UV-index change with the largest deviations in the index most apparent at high latitudes and low longitudes.

Previous analyses of various cyclical signals underlying the variability in total column ozone above five South African cities predicted clear-sky summer erythemal UV-B levels 2.5% to 7.5% higher at midday in the years 1998, 2000 and 2007, this being attributed to the influence of the quasi-biennial oscillation and solar cycle.[7] These predicted future increases in UV-B irradiance were corroborated by our subsequent observations, which indicated enhanced summertime UV-indices in the periods December 1997 to February 1998 and December 2000 to February 2001, ranging between 2.9% and 6.3% above the 23-yr average. The impact of the 11-yr solar cycle on ozone production and consequent surface UV-B irradiance was difficult to substantiate. The largest increases in UV-indices in our study corresponded with periods of low extraterrestrial solar activity and *vice versa* (Table 2), but the ostensible anti-correlation between surface UV-B irradiance and extraterrestrial solar flux was obscured by the large inter-annual variation in UV-index.

Variability in extraterrestrial solar flux increases sharply with decreasing wavelength, and it is the shorter solar (UV-C: <280 nm) wavelengths that control the temperature and photochemistry of the middle atmosphere, including ozone production. Unique measurements of total column ozone above Arosa, Switzerland, from 1900 to 2000 indicate a decline in stratospheric ozone between 1975 and 1980, but the strong fluctuations do not permit detection of other patterns of ozone concentration.[34] However, relationships are evident where these data are compared with solar activity and UV-C radiation. For example, when solar activity is high, so too are solar UV-C radiation and ozone concentrations,[34] the latter known to reduce UV-B radiation reaching the earth's surface.[19] During recent 11-yr solar cycles, irradiance in the UV-C band increased by 2% but the corresponding enhanced solar (not surface) UV-B irradiation was only 0.4%.[34] Measurements in the tropics suggest a change of ~6% in the total column ozone during 11-yr solar cycles from solar low to solar high, whereas estimates from satellite data indicate a total column ozone variation of ~2–3%.[34] On the basis of these ozone changes and a radiation amplification factor (indicating the increase of biologically active radiation with 1% ozone depletion) of ~2.0 to 2.3 for CIE-based erythemal induction between 280 and 315 nm at latitudes 22–35°S, the surface UV-B irradiance could be expected to be ~5–14% higher at the minimum of the 11-yr solar cycle and vice versa over southern Africa. Similarly, our modelled increases in UV-indices associated with the 11-yr solar cycle amplitudes were in the range 4–13% UV-index increase above the 23-yr average at the solar cycle minimum

Table 3. UV-indices, rankings and exposure times based on minimal erythemal doses (MED) for perceptible skin damage in persons of different skin type.

UV-index	Ranking	Minutes to skin damage for different skin types					
		I	II	III	IV	V	VI
		Fair skin, freckles Blond hair Blue eyes Burns easily, peels Tans not	Fair skin, Blond, red hair Blue, hazel eyes Burns easily Tans minimally	Fair skin, Light brown hair Hazel, brown eyes Burns reasonably Tans moderately	Light brown skin Brown, black hair Brown eyes Burns minimally Tans easily and rapidly	Dark brown skin Brown, black hair Brown eyes Burns rarely Tans substantially and immediately	Black skin Black hair Brown eyes Does not burn Tans profusely and immediately
1	Minimal	104.0	140.0	192.0	233.3	285.3	376.0
2	Minimal	52.0	70.0	96.0	116.7	142.7	188.0
3	Low	34.7	46.7	64.0	77.8	95.1	125.3
4	Low	26.0	35.0	48.0	58.3	71.3	94.0
5	Moderate	20.8	28.0	38.4	46.7	57.1	75.2
6	Moderate	17.3	23.3	32.0	38.9	47.6	62.7
7	Moderate	14.9	20.0	27.4	33.3	40.8	53.7
8	High	13.0	17.5	24.0	29.2	35.7	47.0
9	High	11.6	15.6	21.3	25.9	31.7	41.8
10	Very high	10.4	14.0	19.2	23.3	28.5	37.6
11	Very high	9.5	12.7	17.5	21.2	25.9	34.2
12	Very high	8.7	11.7	16.0	19.4	23.8	31.3
13	Acute	8.0	10.8	14.8	17.9	21.9	28.9
14	Acute	7.4	10.0	13.7	16.7	20.4	26.9
15	Extreme	6.9	9.3	12.8	15.6	19.0	25.1
16	Extreme	6.5	8.8	12.0	14.6	17.8	23.5
MED (J cm^{-2})		156	210	288	350	428	564

(Table 2). Such increases were also accompanied by a substantial geographical change in the distribution of the UV-index across southern Africa. For example, during December 1985 and 1997, when solar activity was near its minimum, over 95% of the land area within the borders of South Africa corresponded to a UV-index of 13 and greater under clear skies at midday (Fig. 2B, C) compared to only 2% of the land area in December 1979, when solar activity was close to its maximum (Fig. 2A).

Observed changes in the UV-index associated with the 11-yr solar cycle (Table 2) mostly exceeded long-term upward trends in biologically active UV-B radiation induced by anthropogenic emissions of ozone-depleting trace gases. These upward trends, which were previously inferred from monthly and zonally averaged satellite ozone records between January 1979 and December 1993, indicated annual increases in erythemal active UV-B irradiance over this period ranging from 5.4 ± 1.5% at 25°S to 8.0 ± 1.5% at 35°S.[6] From 1993 onwards, these enhancements in biologically active UV-B irradiance appear to have declined somewhat, since our least-squares regressions revealed an annually averaged increase ($P \leq 0.001$) in UV-B irradiance between January 1979 and December 2001 of only 4.3% (Table 2), though increases as high as 9.0% were apparent in late winter (August). These UV-index increases, though relatively modest, have already caused substantial geographical alteration in the distribution of UV-indices across South Africa, this being apparent from comparisons of their mapped distributions under conditions of maximum solar activity in 1979 with those under comparable levels of solar activity in 2001. Indeed, the comparisons reveal that midday, clear-sky UV-indices of magnitude 13 and greater, which corresponded to only 2% of South Africa's interior in 1979 (Fig. 2A), included as much as 72% of the country's interior in 2001 (Fig. 2D). Such extensive changes are also apparent in coastal areas (Fig. 2A, D) and these are expected to intensify with continuing ozone depletion, especially at the next solar cycle minimum anticipated in 2007/08.

In contrast to UV trends estimated from satellite ozone data, long-term instrument-based measurements of biologically active UV-B irradiance have produced conflicting results. A 12% decrease in erythemal damaging UV-radiation measured by R-B-type meters was reported in Moscow between 1968 and 1983, though this was accompanied by a 13% increase in cloudiness and 15% rise in atmospheric turbidity.[29] Similarly, R-B-type meter measurements taken between 1974 and 1985 at eight different sites in the United States showed decreases in erythemal damaging UV-radiation ranging from 0.5% to 1.1% per year.[26] In contrast, R-B-type meter data obtained at a station in the Swiss Alps (3600 m above sea level at 47°N) indicated enhanced erythemal active UV-radiation of 0.7 ± 0.2% per year between 1981 and 1989, persisting at 0.7 ± 0.3% per year between 1981 and 1991.[30] Likewise, multi-filter measurements taken between 1975 and 1990 at a single site in Maryland, U.S.A., indicated that the maximum monthly mean UV-B irradiance was 13% higher in the period 1983–89 than for the entire data record, though the overall increase of 35% in monthly mean UV-B irradiance recorded from 1977/78 to 1985 was much larger than expected from CFC-induced ozone depletion.[35] These measurements indicate that ozone-induced changes can be detected over a period of several years despite variability due to cloudiness and local pollution. However, linking these entirely to anthropogenic emissions of ozone-depleting trace gases over such relatively short time spans is questionable, especially as many of the above reports of UV-B irradiance increases were ostensibly associated with corresponding decreases in solar activity.

It is expected that, with continued full compliance with the Montreal Protocol and all its amendments, global ozone depletions should peak early in this century with a slow recovery over the next 50 years.[1] Predicted future increases in erythemal active UV-B radiation, based on total column ozone trends between 1979 and 1993, were 15–25% for southern hemisphere mid-latitudes in all seasons.[6] Our approximations, extrapolated from ozone trends between 1979 and 2001, predict future increases in erythemal UV-B irradiance across southern Africa ranging from only 1.9% in early autumn (March) to as much as 24.5% in late winter (August), with an annual average of 11.7%. Such increases, however, should not be treated with complacency, since midday UV-indices during summertime periods of peak recreational sun exposure are already ranked very high to acute

across southern African coastal regions and interior (Fig. 2D). Exposure periods causing perceptible skin damage corresponding to UV-indices of this magnitude range from ~9 min and less in sensitive, fair-skinned persons to ~34 min and less in resilient, dark-skinned subjects (Table 3). These relatively short exposure times point to the importance of scheduling recreational and sporting activities to early or late in the day to limit UV-induced damage to the skin, eyes and immune system.

In conclusion, our observations indicate that increases in the UV-index induced by anthropogenic emissions of ozone-depleting trace gases over southern Africa during the last 23 years have been relatively modest and generally of smaller magnitude than those induced by natural, 11-year oscillations in solar activity. Despite the expected peaking of global ozone depletions early this century, substantially intensified and geographically altered UV-indices may still be expected to occur intermittently in the future where the detrimental effects of residual anthropogenic trace gas emissions on the ozone layer coincide with seasonal ozone troughs and diminished solar activity.

1. WMO (1998). *Atmospheric Ozone. Assessment of Our Understanding of the Processes Controlling its Present Distribution and Change.* World Meteorological Organization, Global Ozone Research and Monitoring Report **44**. Geneva.
2. UNEP (1998). *Environmental Effects of Ozone Depletion: 1998 Assessment.* United Nations Environment Programme, Nairobi.
3. Seckmeyer G., Mayer B., Bernhard G., McEnzie R.L., Johnston P.V., Kotkamp M., Booth C.R., Lucas T., Mestechkina T., Roy C.R., Gies H.P. and Tomlinson D. (1995). Geographical differences in the UV measured by intercompared spectroradiometers. *Geophys. Res. Lett.* **22**, 1889–1892.
4. Zerefos C.S., Balis D., Bais A.F., Gillotay D., Simon P.C., Mayer B. and Seckmeyer G. (1997). Variability of UV-B at four stations in Europe. *Geophys. Res. Lett.* **24**, 1363–1366.
5. McKenzie R.L., Conner B. and Bodeker G.E. (1999). Increased summertime UV radiation in New Zealand in response to ozone loss. *Science* **285**, 1709–1711.
6. Madronich S., McKenzie R.L., Caldwell M.M. and Björn L.O. (1995). Changes in ultraviolet radiation reaching the earth's surface. *Ambio* **24**, 143–152.
7. Bodeker G.E. and Scourfield W.W.J. (1998). Estimated past and future variability in UV radiation in South Africa based on trends in total column ozone. *S. Afr. J. Sci.* **94**, 24–32.
8. Musil C.F. and Bhagwandin N. (1992). The SUN program for computation of solar ultraviolet spectral irradiances: solar exposure limits in South Africa. *S. Afr. J. Sci.* **88**, 406–410.
9. McKinley A.F. and Diffey B.L. (1987). A reference action spectrum for ultraviolet induced erythema in human skin. *Commission Internationale de l'Eclairage Research Note* 6, 17–22.
10. McPeters R.D., Bhartia P.K., Krueger A.J., Herman J.R., Schlesinger B.M., Wellemeyer C.G., Seftor C.J., Jaross G. Taylor S.L., Swissler T., Torres O., Labow G., Byerly W. and Cebula R.P. (1996). Nimbus-7 Data Products User's Guide, NASA Ref. Pub. No. 1384, (PDF file available at http://toms.gsfc.nasa.gov/).
11. Herman J.R., Bhartia, P.K., Krueger A.J., McPeters R.D., Wellemeyer C.G., Seftor C.J., Jaross G. Schlesinger B.M., Torres O., Labow G., Byerly W., Taylor S.L., Swissler T. and Cebula R.P. (1996). Meteor-3 Total Ozone Mapping Spectrometer (TOMS) Data Protocols User's Guide, NASA Ref. Pub. No. 1393, (PDF file available at http://toms.gsfc.nasa.gov/).
12. McPeters R.D., Bhartia P.K., Krueger A.J., Herman J.R., Wellemeyer C.G., Seftor C.J., Jaross G., Torres O., Moy L., Labow G., Byerly W., Taylor S.L., Swissler T. and Cebula R.P., 1998. Earth Probe Total Ozone Mapping Spectrometer (TOMS) Data Products User's Guide, NASA Ref. Pub. (PDF file available at http://toms.gsfc.nasa.gov/).
13. Krueger A.J., Bhartia P.K., McPeters R.D., Herman J.R., Wellemeyer C.G., Jaross G., Seftor C.J., Torres O., Labow G., Byerly W., Taylor S.L., Swissler T. and Cebula R.P. (1998). ADEOS Total Ozone Mapping Spectrometer (TOMS) Data Products User's Guide, NASA Ref. Pub. (PDF file available at http://toms.gsfc.nasa.gov/).
14. Burrows J.P., Weber M., Buchwitz M., Rozanov V., Ladstatter-Weissenmayer A., Richter A., DeBeek R., Hoogen R., Bramstedt K., Eichmann K-U. and Eisinger M. (1999). The Global Ozone Monitoring Experiment (GOME): mission concept and first scientific results. *J. Atmos. Sci.* **56**, 151–175.
15. Musil C.F., Bodeker G.E., Scourfield M.W.J. and Powrie L.W. (2002). All-weather calibration of broadband (Robertson-Berger type) meters for ozone dependency. *S. Afr. J. Sci.* **98**, 397–400.
16. Zar J.H. (1974). *Biostatistical Analysis.* Prentice-Hall, Englewood Cliffs, NJ.
17. Instruction manual: *Model UV-B1 ultraviolet pyranometer.* Yankee Environmental Systems, Turner Falls, MA 01376.
18. Wang P. and Lenoble J. (1994). Comparison between measurements and modeling of UV-B irradiance for clear sky: a case study. *Appl. Optics* **33**, 3964–3871.
19. Stamnes K., Henriksen K. and Ostensen P. (1988). Simultaneous measurements of UV radiation received by the biosphere and total ozone amount. *Geophys. Res. Lett.* **15**, 784–787.
20. McKenzie R.L., Matthews W.A. and Johnston P.V. (1991). The relationship between erythemal UV and ozone, derived from spectral irradiance measurements. *Geophys. Res. Lett.* **18**, 2269–2272.
21. Jokela K., Leszcynski K. and Visuri R. (1993). Effects of Arctic ozone depletion and snow on UV exposure in Finland. *Photochem. Photobiol.* **58**, 559–566.
22. McKenzie R.L., Kotkamp M., Seckmeyer G., Erb R., Roy C.R., Gies H.P. and Toomey S.J. (1993). First southern hemisphere intercomparison of measured solar UV spectra. *Geophys. Res. Lett.* **20**, 2223–2226.
23. Zheng X. and Basher R.E. (1993). Homogenisation and trend detection analysis of broken series of solar UV-B data. *Theor. Appl. Climatol.* **47**, 189–203.
24. Zeng J., McKenzie R., Stamnes K., Wineland M. and Rosen J. (1994). Measured UV spectra compared with discrete ordinate method simulations. *J. Geophys. Res.* **99**, 23019–23030.
25. Cunningham P.F. and Bodeker G.E. (2000). Ground-based measurements of UV-B in Namibia. *S. Afr. J. Sci.* **96**, 547–549.
26. Scotto J., Cotton G., Urbach F., Berger D. and Fears T. (1988). Biologically effective ultraviolet radiation: surface measurements in the United States, 1974–1985. *Science* **239**, 762–764.
27. Scotto J., Fears T. and Gori G.B. (1975). Measurements of ultraviolet radiation in the United States and comparisons with skin cancer data. U.S. Dept. of Health, Education, and Welfare, Report No. (NIH) 76-1029. Washington, D.C.
28. Cotton G.F. (1990). Robertson-Berger UVB meter: In: *Summary Report 1989, Climate Monitoring and Diagnostics.* Report No. 18, National Oceanic and Atmospheric Administration, Boulder, Colorado..
29. Garadzha, M.P. and Nezval Ye. I. (1987). Ultraviolet radiation in large cities and possible ecological consequences of its changing flux due to anthropogenic impact. In *Proc. Symposium on Climate and Human Health,* pp. 64–68. World Climate Applications Programme, WCAP Report No. 2, Leningrad.
30. Blumthaler M. and Ambach W. (1990). Indications of increasing solar ultraviolet-B radiation flux in Alpine regions. *Science* **248**, 206–208.
31. Ilyas M. (1987). Effect of cloudiness on solar ultraviolet radiation reaching the surface. *Atmos. Env.* **21**, 1483–1484.
32. Cabrera S., Bozzo S. and Fuenzalida H. (1994). Variations in UV radiation in Chile. *J. Photochem. Photobiol.* **28**, 137–142.
33. Blumthaler M. (1993). Solar UV measurements. In *Environmental Effects of UV (Ultraviolet) Radiation,* ed. M. Tevini, pp. 17–69. Lewis Publisher, Boca Raton, Florida.
34. Rozema J., van Geel B. and Björn L.O. (2002). Towards solving the UV puzzle. *Science* **296**, 1621–1622.
35. Correll D.L., Clark C.O., Goldberg B., Goodrich V.R., Hayes D.R., Klein W.H. and Schecher W.D. (1992). Spectral ultraviolet-B radiation fluxes at the earth's surface: long-term variations at 39°N, 77°W. *J. Geophys. Res.* **97**, 7579–7591.